A rational approach to noise discrimination in video microscopy particle tracking

Thierry Savin,[1] Patrick T. Spicer,[2] and Patrick S. Doyle[3,a)]
[1]*School of Engineering and Applied Sciences, Harvard University, Cambridge, Massachusetts 02138, USA*
[2]*The Procter & Gamble Company, Corporate Engineering, West Chester, Ohio 45069, USA*
[3]*Department of Chemical Engineering, Massachusetts Institute of Technology, Cambridge, Massachusetts 02139, USA*

(Received 28 February 2008; accepted 21 June 2008; published online 14 July 2008)

The authors describe a rational approach to an important step in video microscopy particle tracking called noise discrimination. Using the morphology of the brightness profiles produced by the particles, false and dubious detections are eliminated from the valid tracking data. This selection process is found to affect the spatial resolution ε and the depth z_b of the tracking. Accordingly, it is shown that a stringent selection of the particles closest to the focal plane improves the spatial resolution (i.e., decreases ε) but also diminishes z_b. The authors further demonstrate that the statistical accuracy is worsened by lower z_b. Noise discrimination thus has a critical influence on the overall performance of the particle tracking technique. © *2008 American Institute of Physics*. [DOI: 10.1063/1.2957464]

Multiple particle tracking (MPT) using video microscopy is a popular technique that permits the simultaneous measurements of ~100 probe trajectories. It is now routinely applied in various fields of research, from fundamental colloidal physics[1] to force measurements in biological systems.[2] In typical experiments, videos of moving probes dispersed in a sample are acquired using a charge-coupled device (CCD) camera attached to a fluorescent microscope. The signal emitted by the fluorescent particles in each movie frame then consists of multiple bright circular spots on a dark background.[3,4] The majority of MPT experiments rely on the movie processing algorithms developed by Crocker and Grier.[3] Their procedures locate the positions of the brightness profiles created by the particles in each frame of the digitized movie. Morphological characteristics of these profiles are concomitantly calculated, and are used to remove false and dubious detections (such as aggregates of particles or misidentified noise) in an intermediate step called "noise discrimination." Thereafter, the positions of the remaining features are connected to each other in successive frames to form trajectories. In this letter we describe a rational route to perform noise discrimination and emphasize how it affects both the spatial resolution ε and the depth of tracking z_b. This step is thus critical because ε and z_b are known to impact the MPT performance at low and high lag times, respectively.[4,5]

Within a single image (filtered beforehand by smoothing and background subtraction[3]), the MPT algorithms compute the moments of each spot's brightness distribution. The signal-weighted locations of the particles on the CCD pixel array are thus calculated, along with the integrated brightness s, the profile's radius of gyration r, and the eccentricity e of their images (from 0 for a circle to 1 for an elongated spot). After these measurements are performed on all frames, the resulting raw data collected from all candidate features are clipped by selecting the correct ranges for (s,r,e) to avoid the inclusion of spurious particles in the subsequent tracking steps.[6,7] For example, if an aggregate of two particles is detected as a single feature, the values (s,r,e) calculated from its profile will supposedly lie well outside a target cluster of points corresponding to "normal" features.[3,6] We begin here by evaluating this target cluster of valid points as used for noise discrimination in fluorescence microscopy MPT.

When a particle visits different altitudes z in the direction normal to the imaging plane, the total brightness and the radius of its image greatly vary (cf. Fig. 1; the eccentricity was found to remain essentially unchanged and is not shown here). These morphological changes are mainly consequences of diffraction and spherical lens aberration,[8] and can be used to perform three-dimensional tracking after a proper calibration.[3,9,10] In order to experimentally evaluate the evolution of $s(z)$ and $r(z)$ as a function of z, we immobilized probes in an agarose gel of concentration 1 wt %. The agarose (Seakem LE; BMA) was dissolved in boiling water, and 0.925 μm diameter fluorescent beads (Polysciences) were added at 80 °C during cooling. A custom-built chamber of observation was loaded with the hot solution and sealed with vacuum grease. Upon further cooling to room temperature, the agarose solution forms a gel that constrains the particles to motions well below the tracking limit of detection. Also, we note that agarose has the same refractive index as water.[11] By attaching the microscope focusing knob to a motor, a 40× objective lens (Zeiss; numerical aperture 0.75) was translated in the z direction away from the sample holder, at a constant velocity $v=15\pm0.5$ μm s^{-1}, while a focus scan movie of the dispersed particles was acquired at 30 fps. We applied the MPT algorithms on the deinterlaced movie at times when the translating volume of observation was between 30 and 70 μm above the bottom of the chamber. We visually checked the validity of the found features by overlaying their locations with the original microscope images, and we manually removed obvious false hits. For all trajectories, $s(t=z/v)$ passes through a maximum value $s_{\max}$ at an altitude that we set to 0, and that defines the focal plane (see Fig. 1). All curves $s(z)$, $r(z)$, and $e(z)$ then overlapped to within 10% of their respective constant-z ensemble mean

a)Electronic mail: pdoyle@mit.edu.

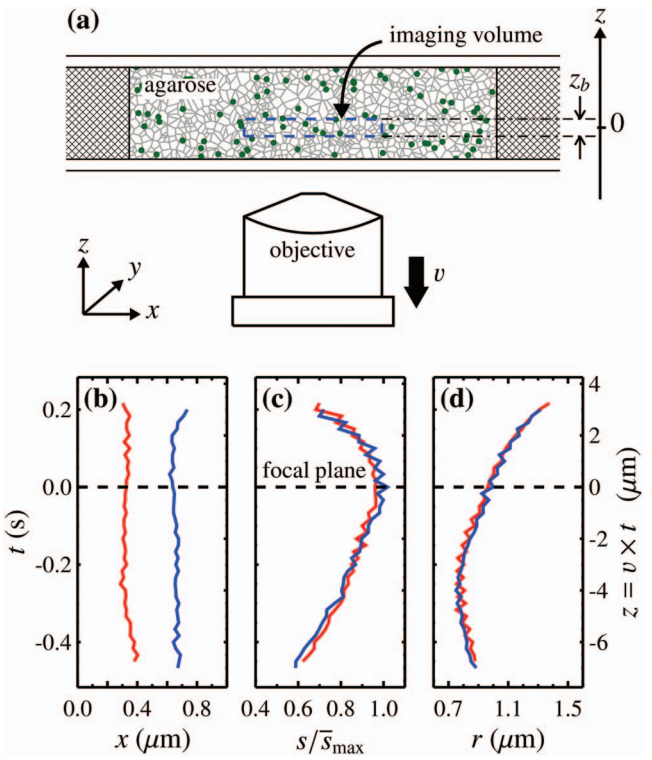

FIG. 1. (Color) (a) Schematic for the experiments used to assess the variation of s and r with the altitude z. Shown in (b) are two typical x-trajectories while (c) and (d) show the curves $s(z)$ and $r(z)$, respectively, for the two particles (their altitudes of maximum brightness were matched at $z=0$).

$\bar{s}(z)$, $\bar{r}(z)$, and $\bar{e}(z)$, even if our visual preselection was significantly less restrictive. Variations around the mean mainly come from camera artifacts.[4] The curves end at altitudes defining the intrinsic imaging depth of the instrument, out of which the particle images are discarded by filtering. We show in Fig. 2 typical images and the resulting path $\mathcal{P}:(s(z),r(z))$ acquired when the particle travels in the z direction across the imaging volume. Also shown in Fig. 2 is the average curve $\bar{\mathcal{P}}:(\bar{s}(z),\bar{r}(z))$ we calculated from 200 trajectories. The shape of $\bar{\mathcal{P}}$ depends on the instrumentation: microscope optics, size of beads and tracking parameters, altitude of the focal plane in the sample, etc. However, the variations of $s(z)$ and $r(z)$ usually conform to the following trends: an asymmetric increase of r and drop of s on both sides of the focal plane. As a result, $\bar{\mathcal{P}}$ is often a "loop" similar to the one seen in Fig. 2.

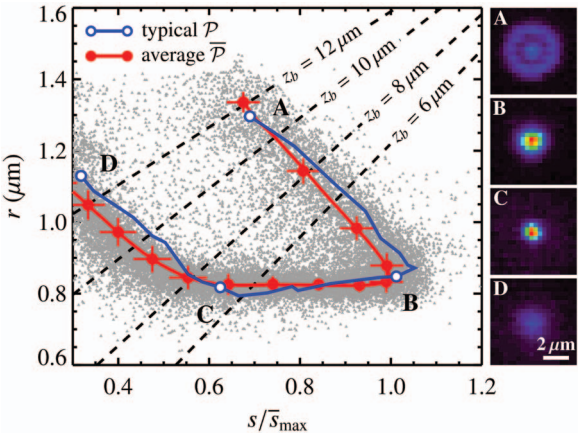

FIG. 2. (Color) Tracking data in the (s,r) morphological parameter space used for noise discrimination. The curve $\mathcal{P}$ is a typical path from a probe uniformly moving in the z direction, as measured in the agarose experiment. The four circles labeled A, B, C, and D along $\mathcal{P}$ correspond to the four fluorescence images on the right hand side (the particle is at the top z-edge of the imaging volume in A, and at the bottom in D). The curve $\bar{\mathcal{P}}$ is the average over 200 of such paths $\mathcal{P}$. The dots on $\bar{\mathcal{P}}$ designate 1 μm increments of z, and the error bars specify the standard deviations $\bar{\sigma}_{\mathcal{P}}=(\bar{\sigma}_s,\bar{\sigma}_r)$. The points scattered around $\bar{\mathcal{P}}$ are from features detected by MPT measurements in water. The dashed lines define clipping regions for dubious data removal.

TABLE I. Values of the tracking depth z_b and of the spatial resolution ε as determined by using (1) fixed particles, (2) particles' concentration, and (3) trajectory durations.

$z_b^{(1)}$ (μm)	$z_b^{(2)}$ (μm)	$z_b^{(3)}$ (μm)	$\varepsilon^{(1)}$ (nm)	$\varepsilon^{(2)}$ (nm)
6 ± 1	6.0 ± 0.5	5.2 ± 0.4	9 ± 1	12 ± 7
8 ± 0.9	8.2 ± 0.5	6.7 ± 0.5	10 ± 1	14 ± 5
10 ± 0.9	10.7 ± 0.5	8.3 ± 0.8	11 ± 1	13 ± 5
12 ± 0.8	12.9 ± 0.5	9.5 ± 1	12 ± 1	15 ± 4

Discarding particles at the edges of the intrinsic imaging volume (i.e., around the ends of $\bar{\mathcal{P}}$) is a required thresholding that ensures the elimination of dubious signal.[7] When clipping the cluster of points in the (s,r) plane, it is moreover preferable to achieve the best spatial resolution in the consequent tracking. To determine the clipping region, we first set a value z_b of tracking depth and chose two altitudes z_1 and $z_2=z_1+z_b$, to which correspond two points $(s,r)_1$ and $(s,r)_2$ on the average path $\bar{\mathcal{P}}$. Selecting particles at $z\in[z_1,z_2]$ means discarding all features above the line connecting the points $(s,r)_1$ and $(s,r)_2$ (see Fig. 2). From the tracking performed with the remaining selected features, we evaluated the spatial resolution ε using the one-dimensional mean-squared displacement (MSD) of the fixed particles,[4] $\langle\Delta x^2\rangle=2\varepsilon^2$. For a given z_b, several clipping lines can be constructed and we choose the one that minimizes ε. In our experiment, we applied this method to determine the clipping lines shown in Fig. 2 for the parameters $z_b=6$, 8, 10, and 12 μm (the optical depth of field of the objective is 5.2 μm, as given by the manufacturer). We report in Table I the resulting minimum values of ε obtained by this method [labeled (1) in the table]. Most notably, we observe that the spatial resolution worsens with an increasing tracking depth.

To compare these results with a routine experiment, we performed 30 s tracking of $d=0.925$ μm diameter polystyrene beads dispersed in a 1:1 solution of H_2O/D_2O (polystyrene density matching) at a volume fraction $\phi=2.6\times10^{-3}\%$. The instrumentation was identical to the one used in the fixed-particle experiment, and the volume of observation was 50 μm above the bottom of the chamber. After a visual preselection of valid features, the clipping ranges for (s,r) were chosen identical to the agarose experiment for the different values of z_b investigated here. We repeated this experiment 20 times and combined our measurements into one tracking array to improve statistical accuracy. We show in Fig. 2 the resulting (s,r) scatter plot prior to clipping, and observe a good agreement with the average curve $\bar{\mathcal{P}}$. Knowledge of the beads' concentration $C_b=6\phi/(\pi d^3)$ was used to obtain an independent measure of z_b. The total instantaneous number $N_b(t)$ of tracked particles in each frame is a fluctuating variable with time average $\langle N_b\rangle$ and a standard devia-

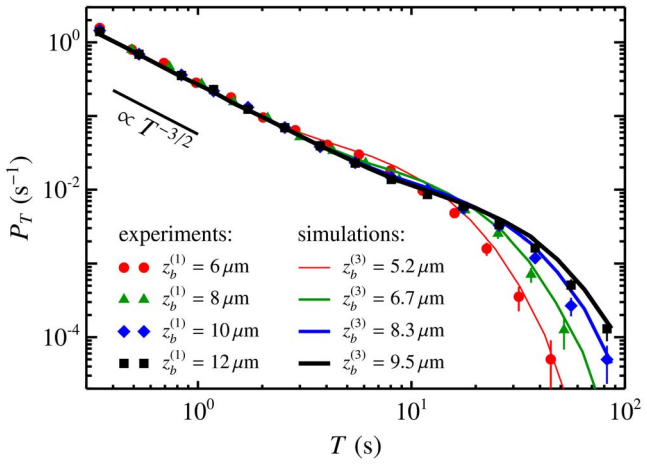

FIG. 3. (Color online) PDF of trajectory durations from 0.925 μm diameter MPT measurements in a 1:1 solution of H_2O/D_2O.

tion that we found to be less than 5% of the mean. From $\langle N_b \rangle = C_b x_b y_b z_b$, where $x_b \times y_b$ is the known camera field of view, we calculated a value $z_b^{(2)} = \langle N_b \rangle / (C_b x_b y_b)$ for each clipping input parameter z_b. We report these values in Table I and observe a good agreement with the previous estimation. Note that this method (2) does not depend on the particular dynamics of the particles. It depends, however, on the concentration C_b, unlike method (1), ensuring that $z_b^{(1)}$ and $z_b^{(2)}$ are two independent estimates. Moreover, we can calculate the spatial resolution from the zero lag time intercept of the particles' MSD in the viscous fluid.[4] The estimates $\varepsilon^{(2)}$ presented in Table I are affected by a large uncertainty that increases for lower z_b due to statistical limitations explained below. Nevertheless $\varepsilon^{(2)}$ remains close to the static evaluation $\varepsilon^{(1)}$.

The statistical accuracy of estimators calculated from the trajectories is related to the tracking depth.[5] To illustrate this effect, we plot in Fig. 3 the probability density function (PDF) P_T of the trajectory duration T as measured in the viscous fluid employed above for various clipping parameters z_b. We see that short tracks are more frequently observed. The power-law scaling $\propto T^{-3/2}$ measured at small T is typical of first-return time distribution,[12] since these short trajectories are predominantly coming from particles entering and leaving the imaging volume by the same constant-z edge. As z_b decreases, particles are less likely to reside in the tracking volume for long times. Thus at large lag times, the accuracy of statistical estimates (such as the MSD), calculated from the rarefied long tracks, worsens.[5] For completeness, we used a Brownian dynamics simulation that takes the finite imaging volume into account to calculate the PDF of trajectory durations in a similar viscous fluid (see details in Ref. 5). We plot in Fig. 3 the results of these simulations performed with the values $z_b^{(3)}$ found to best match (i.e., minimum chi-square) our experimental results. We report in Table I the values of z_b obtained by this method (3). We observe that they are of the same magnitude as the ones measured experimentally, although they are consistently smaller. This is likely due to missing positions when building trajectories from experimental data. Indeed, particles in the observation volume can still be briefly discarded if, for instance, their images overlap or get affected by camera noise. Because of a missed position, a trajectory is cut into two shorter tracks resulting in a PDF of durations that is biased toward smaller apparent z_b, as observed in our results.

In order to perform efficient MPT measurements, we propose to predetermine the ranges of valid (s,r) data for noise discrimination by tracking particles fixed in an agarose gel. This preliminary experiment also allows one to precisely evaluate both ε (from the MSD) and z_b (from the known beads' concentration in the gel) after choosing the clipped cluster of (s,r) points. The resulting idealized scatter plot and clipping region can then be employed to discriminate noise in further experiments that utilize the same instrumentation. When clipping, we showed that performing a stringent selection of features close to the focal plane improves the spatial resolution ε, at the expense of degrading the statistical accuracy limited by lower z_b. However, when average quantities are sought from the tracks, the maximization of z_b will be prioritized since corrections for a finite spatial resolution are then possible.[4] Along with our previous methods,[4,5] we thus recommend to apply this rational procedure in future MPT measurements.

The authors acknowledge support from the Procter & Gamble Company.

[1] D. S. V. Prasad and E. R. Weeks, J. Phys.: Condens. Matter **19**, 113102 (2007).
[2] D. Weihs, T. G. Mason, and M. A. Teitell, Phys. Fluids **19**, 103102 (2007).
[3] J. C. Crocker and D. G. Grier, J. Colloid Interface Sci. **179**, 298 (1996).
[4] T. Savin and P. S. Doyle, Biophys. J. **88**, 623 (2005).
[5] T. Savin and P. S. Doyle, Phys. Rev. E **76**, 021501 (2007).
[6] I. F. Sbalzarini and P. Koumoutsakos, J. Struct. Biol. **151**, 182 (2005).
[7] J. C. Crocker and B. D. Hoffman, *Cell Mechanics*, Methods in Cell Biolgy, Vol. 83 (Elsevier, San Diego, CA, 2007), pp. 141–178.
[8] S. Inoué and K. R. Spring, *Video Microscopy: The Fundamentals*, 2nd ed. (Plenum, New York, 1997).
[9] M. Speidel, A. Jonáš, and E. L. Florin, Opt. Lett. **28**, 69 (2003).
[10] M. Wu, J. W. Roberts, and M. Buckley, Exp. Fluids **38**, 461 (2005).
[11] S. Hell, G. Reiner, C. Cremer, and E. H. K. Stelzer, J. Microsc. **169**, 391 (1993).
[12] M. Ding and W. Yang, Phys. Rev. E **52**, 207 (1995).